


## ORIGINAL INVESTIGATION

# Ultrasonographic findings associated with normal pregnancy and fetal well-being in the bottlenose dolphin (*Tursiops truncatus*)

Marina Ivančić<sup>1</sup>  | Forrest M. Gomez<sup>2</sup> | Whitney B. Musser<sup>2</sup> | Ashley Barratclough<sup>2</sup> | Jennifer M. Meegan<sup>2</sup> | Sophie M. Waitt<sup>3</sup> | Abraham Cárdenas Llerenas<sup>4</sup> | Eric D. Jensen<sup>5</sup> | Cynthia R. Smith<sup>2</sup>

<sup>1</sup>Chicago Zoological Society, Brookfield Zoo, Brookfield, Illinois

<sup>2</sup>National Marine Mammal Foundation, San Diego, California

<sup>3</sup>University of Southern California, Los Angeles, California

<sup>4</sup>Dolphin Adventure, Nuevo Vallarta, Mexico

<sup>5</sup>US Navy Marine Mammal Program, San Diego, California

## Correspondence

Marina Ivančić, Chicago Zoological Society, Brookfield Zoo, Brookfield, IL, USA.

Email: marina.ivancic@czs.org  
Cynthia Smith, National Marine Mammal Foundation, San Diego, CA, USA.  
Email: cynthia.smith@nmmf.org

## Funding information

Gulf of Mexico Research Initiative, Grant/Award Number: SA 16-17

## Abstract

Reproductive success is vital in sustaining free-ranging and managed bottlenose dolphin (*Tursiops truncatus*) populations. Ultrasonography is an invaluable, non-invasive tool in assessing the fetomaternal unit in humans and animals, including dolphins and horses. The purpose of this prospective longitudinal cohort study was to develop a protocol for fetomaternal ultrasonographic monitoring in dolphins and to report normal measurements and descriptive findings correlated with a positive outcome. From 2010 to 2017, serial ultrasonographic evaluations of 12 healthy dolphins were performed over the course of 16 pregnancies. A total of 203 ultrasound examinations were included in the study. Several metrics were accurate in predicting fetal age. Fetal biparietal diameter (BPD), thoracic width in dorsal and transverse planes, thoracic height in a sagittal plane, aortic diameter, and blubber thickness all demonstrated high correlation with gestational age ( $r > 0.94$ ,  $P < .00001$ ). Regional uteroplacental thickness significantly increased with each trimester (range 0.22–0.40 cm;  $P < .00011$  cranial uterus,  $P < .00057$  mid, and  $P < .000011$  caudal). Lung:liver mean pixel intensity was  $2.57 \pm 0.46$  (95% confidence interval 2.47–2.67). Ultrasonographic characteristics of normal pregnancy in dolphins are described and an equation for prediction of parturition date in *Tursiops* is reported: days to parturition =  $348.16 - (26.03 \times \text{BPD}(\text{cm}))$  ( $R^2 = 0.99$ ). Future applications of these normal data will help identify in utero abnormalities indicative of fetal morbidity, and improve understanding of reproductive failure in wild and managed populations.

## KEYWORDS

development, fetus, gestation, marine mammal, ultrasound

## 1 | INTRODUCTION

Ultrasonographic evaluation of pregnancy is a valuable non-invasive diagnostic tool, well-established in human and veterinary medicine. Advances in human perinatology and maternal-fetal medicine have been shown to reduce morbidity and mortality,<sup>1</sup> and fetomaternal

ultrasound is vital in monitoring pregnancy and maximizing neonatal survival.<sup>2</sup> Ultrasound is also a critical component of bottlenose dolphin (*Tursiops truncatus*) medicine and has been used to evaluate pulmonary, cardiac, reproductive, hepatic, urinary, gastrointestinal, and lymphatic systems.<sup>3–9</sup> Improved understanding of *Tursiops* reproduction through routine imaging in managed care has led to advancements

Abbreviations: BPD, biparietal diameter; CL, corpus luteum; MPI, mean pixel intensity.

EQUATOR network guidelines disclosure: The authors followed ARRIVE reporting guidelines.

Previous presentation or publication disclosure: A portion of these findings were presented by M. Ivančić at the 51st American Association of Zoo Veterinarians Annual Conference in September 2019, and by C. Smith at the World Marine Mammal Conference in December 2019.

This is an open access article under the terms of the Creative Commons Attribution-NonCommercial-NoDerivs License, which permits use and distribution in any medium, provided the original work is properly cited, the use is non-commercial and no modifications or adaptations are made.

© 2020 National Marine Mammal Foundation. *Veterinary Radiology & Ultrasound* published by Wiley Periodicals, Inc. on behalf of American College of Veterinary Radiology

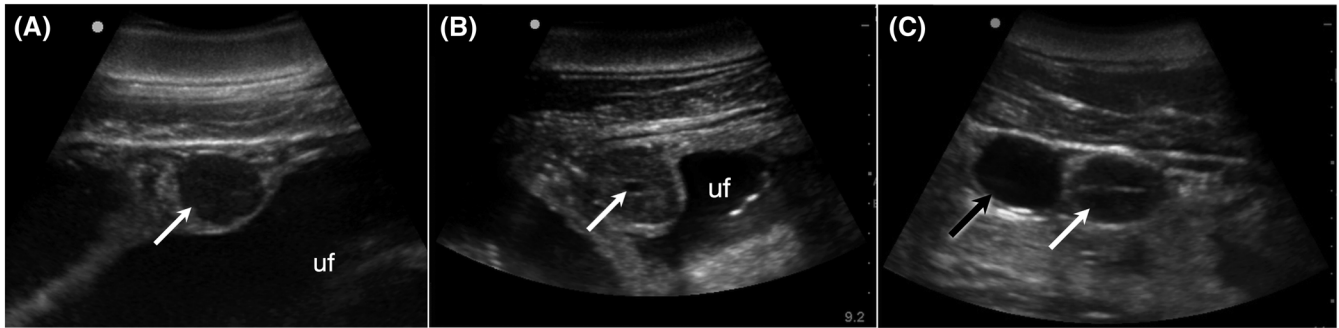


**FIGURE 1** A, Solid corpus luteum (CL) of pregnancy (arrow); uf, uterine fluid. B, Central cavitation in CL (arrow). C, Ovarian cyst-like structure (black arrow) near solid CL (white arrow) (2-5 MHz curvilinear transducer)

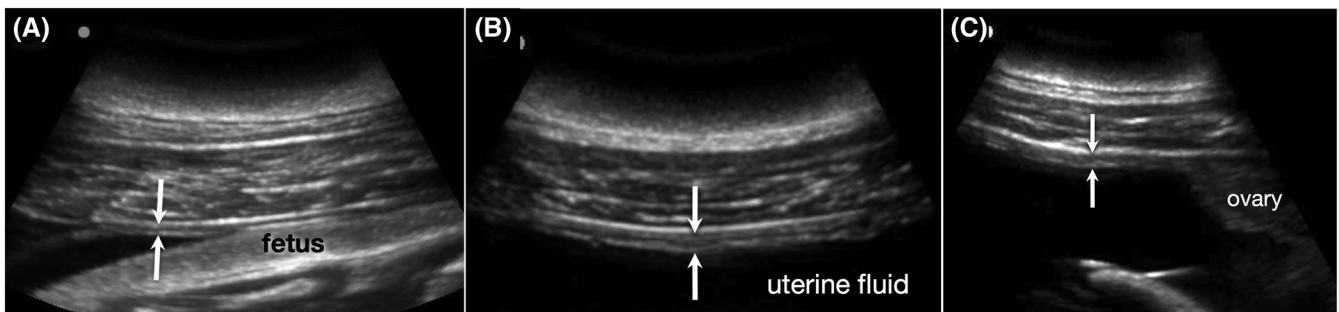


**FIGURE 2** Uteroplacental unit (UPU) thickness in the A, cranial; B, mid; and C, caudal uterus. Arrows indicate the margins of each measurement. Cranial is to the left of each image. A shallow depth setting is used, typically  $\leq 11$  cm (2-5 MHz curvilinear transducer)

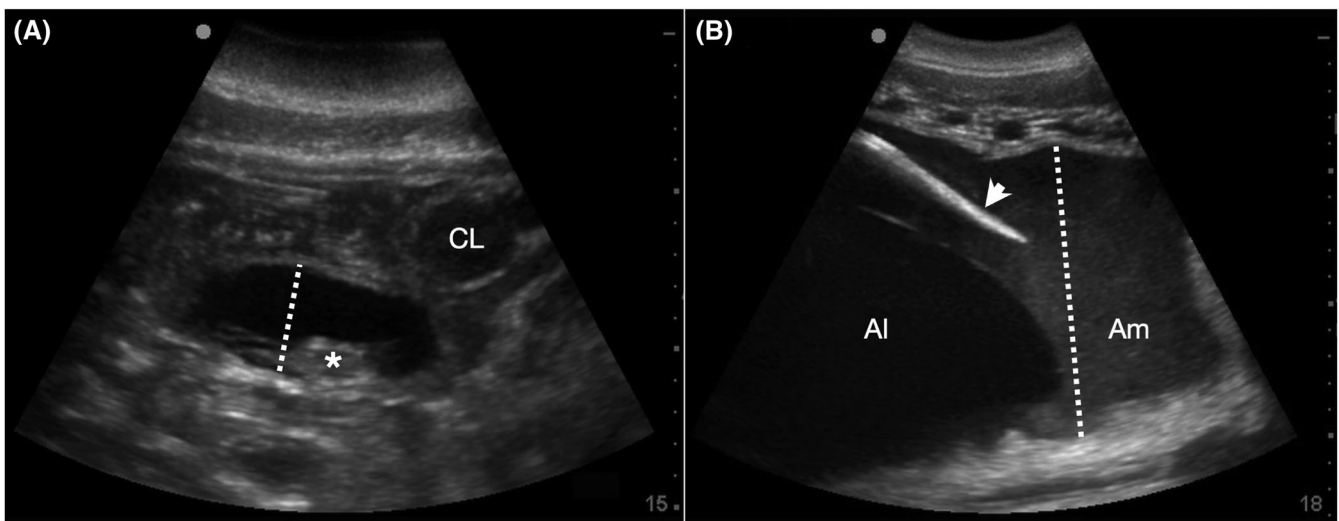


**FIGURE 3** A, Small volume of anechoic uterine fluid, early pregnancy. Allantoic and amniotic fluid compartments are undistinguishable. Dotted line = max fluid depth, \* = embryo, CL = corpus luteum. B, Large volume of uterine fluid, mid-late pregnancy. AI = anechoic allantoic fluid, Am = echogenic amniotic fluid, dotted line = max depth of amniotic fluid, arrowhead = fetal pectoral flipper (2-5 MHz curvilinear transducer)

in hormone analysis, gonadal evaluation, early fetal monitoring, parturition prediction, and artificial insemination.<sup>10-13</sup> This knowledge has successfully been applied to longitudinal investigations of wild dolphin health.<sup>14</sup>

A number of congenital lesions have been reported in *Tursiops* fetuses and perinates, including umbilical cord abnormalities,<sup>15,16</sup> vascular pathologies,<sup>17</sup> and cranial malformations.<sup>18</sup> Following the “Deepwater Horizon” oil spill in 2010, wild dolphins living in

oil-impacted bays had increased prevalence of perinatal mortality, fetal distress, fetal pneumonia,<sup>19</sup> and maternal pulmonary disease and reproductive failure.<sup>20-22</sup> The most likely cause of these abnormalities was exposure to petroleum products.<sup>23,24</sup> To better understand these findings, promptly diagnose congenital anomalies, and enhance early detection of pregnancy complications in wild and managed dolphins, there is a need for more sophisticated assessments of fetoplacental health.

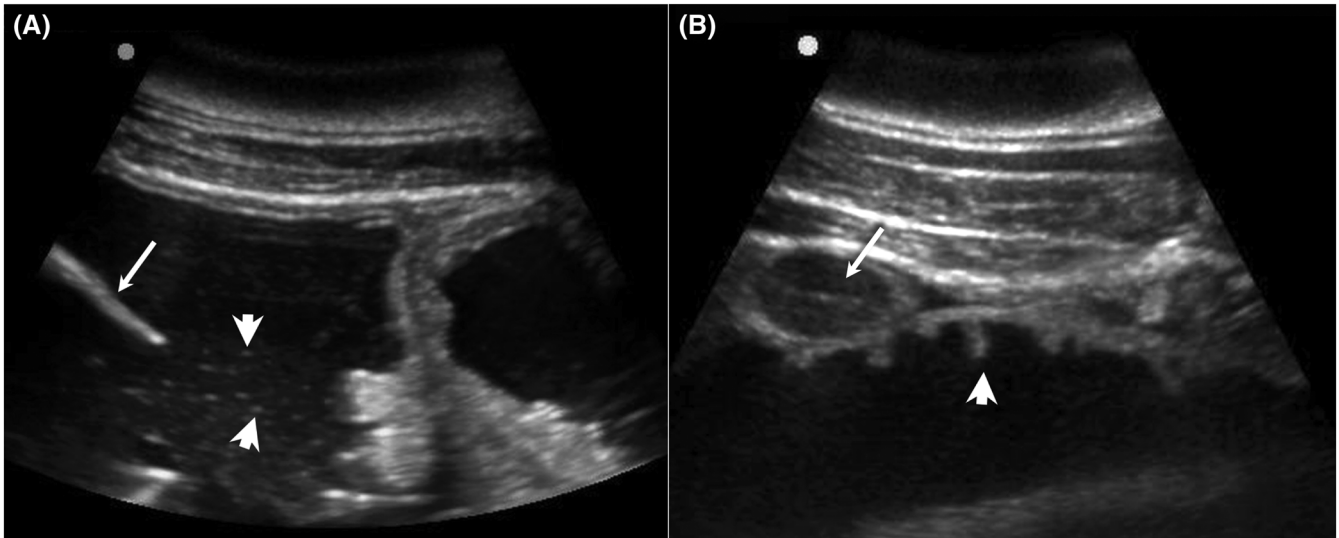


**FIGURE 4** A, Hyperechoic free-floating particles (arrowheads) occasionally seen in amniotic fluid; arrow = fetal pectoral flipper. B, Roughing/frond-like projections (arrowhead) extending from uterine wall; arrow = corpus luteum (2-5 MHz curvilinear transducer)

Standard ultrasonographic methodology to assess fetal growth and well-being has been established in humans and horses.<sup>25-28</sup> Such evaluations help predict positive versus negative outcomes and aid in understanding of pregnancy failure pathophysiology.<sup>29-31</sup> As dolphins and horses have a similar diffuse epitheliochorial placenta, equine reproductive ultrasound provides a reasonable species model.<sup>32,33</sup> The purpose of this study was to expand upon early work in gestational ultrasound of bottlenose dolphins<sup>34-36</sup> and develop a reproducible protocol for ultrasonographic monitoring of fetomaternal health in the bottlenose dolphin, reporting normal measurements and descriptive findings correlating with a positive outcome.

## 2 | MATERIALS AND METHODS

### 2.1 | Study population

In this prospective, longitudinal cohort study, serial voluntary transabdominal ultrasonography was performed on 12 healthy pregnant dolphins during the course of 16 successful pregnancies. Reproductive success was defined as delivery of a calf that survived  $\geq 30$  days. Dams ranged in age from 9 to 46 years old at parturition. They were considered in good health by licensed clinical marine mammal veterinarians based on routine blood work, ultrasonography, and absence of clinical signs throughout pregnancy. Ten dolphins were evaluated at the US Navy Marine Mammal Program in San Diego, California and two at Dolphin Adventure in Puerto Vallarta, Mexico. The US Navy Marine Mammal Program is accredited by the Association for Assessment and Accreditation of Laboratory Animal Care International and adheres to the national standards of the US Public Health Service Policy on the Humane Care and Use of Laboratory Animals and the Animal Welfare Act. Its animal care and use program is reviewed by an Institutional Animal Care and Use Committee and the Department of Defense Bureau of Medicine, as required by the Department of Defense.

### 2.2 | Ultrasonography techniques

Examinations were performed by one of four clinical marine mammal veterinarians (C.R.S., 20 years of experience in dolphin medicine and ultrasonography; F.M.G., 10 years; J.M.M., 10 years; or A.C.L., 4 years) using a portable ultrasound unit (SonoSite Edge, SonoSite, Bothell, Washington, or GE Voluson *i*, General Electric Healthcare, Chicago, Illinois) and a 2-5 MHz curvilinear transducer. Lateral and ventral abdominal scanning was performed using seawater for acoustic coupling. The dolphin voluntarily rested at the surface. Monthly ultrasound examinations began at pregnancy diagnosis. Most evaluations adhered to a detailed fetomaternal ultrasound datasheet. Near estimated parturition dates, cursory examinations assessing fetal viability were performed more frequently. Cine loops capturing multiple areas of interest were recorded when possible to minimize examination duration. Images were qualitatively and quantitatively evaluated retrospectively with DICOM viewing software (OsiriX MD, Pixmeo, Geneva, Switzerland) by an undergraduate research student (S.M.W.) and a research assistant with an MS degree (W.B.M.) under detailed guidance from clinicians (C.R.S., F.M.G.) and an American College of Veterinary Radiology-certified veterinary radiologist (M.I.) with 18 years of experience in clinical marine mammal imaging. Clinicians (C.R.S., F.M.G., J.M.M., A.C.L.) were not blinded regarding individual animal reproductive history. Two observers (W.B.M. and M.I.) were aware that each gestational dataset included was associated with a successful reproductive outcome.

Total ovarian follicle number, largest follicular diameter, maximum orthogonal dimensions of the corpus luteum (CL), and presence of CL cavitation were noted (Figure 1). If anechoic ovarian structures were repeatedly found, total number and maximum orthogonal dimensions of these cysts were noted.

The uteroplacental unit represents the fusion of the uterine wall and diffuse placenta. Thickness was measured from both sides of the animal in three locations (Figure 2): the most cranial margin in

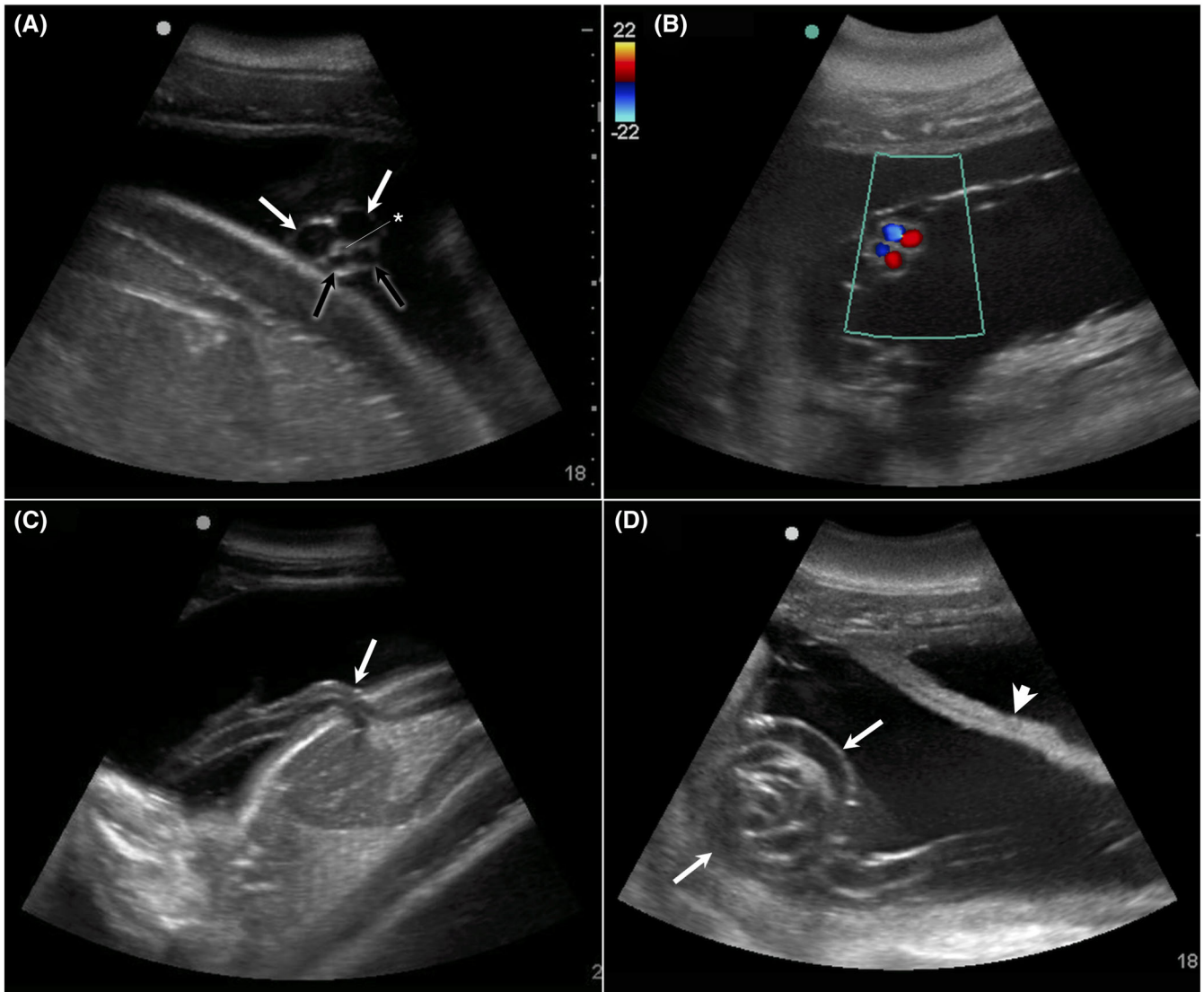


**FIGURE 5** A, Transverse view of umbilicus; white arrows = 2 umbilical veins; black arrows = 2 umbilical arteries. Faint hypoechoic central cavity is the urachus (\*). B, Color Doppler demonstrating flow within the umbilical vasculature. C, Sagittal view of fetal insertion of the umbilicus; fetal ventrum is in the near field and head is in the left far field. D, Loose ball-shaped coil of the cord (arrows) that resolved on re-evaluation; arrowhead = uterine wall fold (2-5 MHz curvilinear transducer) [Color figure can be viewed at [wileyonlinelibrary.com](http://wileyonlinelibrary.com)]

contact with the dam's body wall (Cranial), just cranial to the normal broadening seen near the ovary (Caudal), and the subjective midpoint (Mid) between these. "Mid" was not measured during the first trimester, given small uterine size. Thickness between the ovary and cervix was not measured due to heavy uterine folding normally present in the caudally tapered dolphin abdomen. Minimum and maximum measurements were obtained in triplicate at each location, separated by 0.5 cm in the first trimester and 1.0 cm thereafter. Care was taken to ensure neither the abdominal musculature nor the amniotic membrane was included. Areas of fetal contact/stretched uterine wall were avoided. In late gestation, ballottement created a transient space between the uterus and fetus for measurement. The uterus was critically evaluated for hypo-/anechoic disruptions in uteroplacental contact, distinguishable from uterine vasculature with color Doppler.

Maximum uterine fluid depths were measured (Figure 3). Allantoic depth was measured from the internal surface of the uteroplacental

unit to the near margin of the amnion or the deep margin of the allantois, whichever depth was greater. Amniotic depth was the maximum height of fluid surrounding the fetus, perpendicular to the long axis of the cavity. Fluid echogenicity was assessed as anechoic, hypoechoic, or hyperechoic, and the presence of echogenic free-floating particles (FFPs) was noted (Figure 4A). When a distinction between amniotic and allantoic compartments could not be made, the maximal depth and echogenicity of uterine fluid and presence of FFPs were noted.

Umbilical cord vasculature and urachal conspicuity were assessed in cross section (Figure 5). Color Doppler confirmed vascular flow. Maximum cord diameter near the fetal insertion was measured when seen.<sup>37,38</sup> Cord vessel number and symmetry were assessed, and flattening, convolution/tangling,<sup>39</sup> or coiling noted. Fetal movement was subjectively graded as none, rare, frequent, or continuous.

Biparietal diameter (BPD) was measured in a dorsal plane in which the head was divided into dorsal and ventral segments and the *falx*



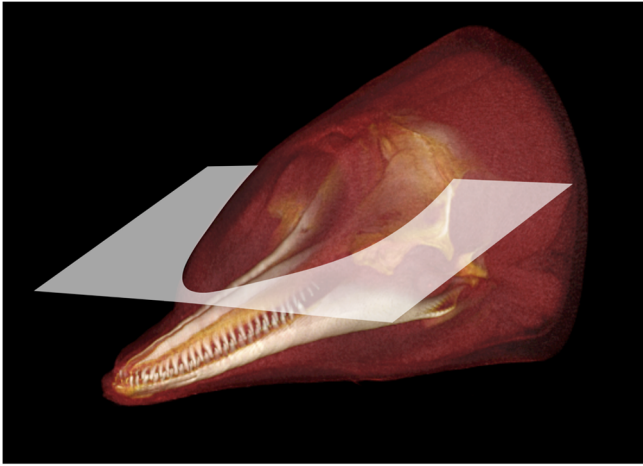


**FIGURE 6** An archived head CT scan of a live *Tursiops* was used to create a 3D volume rendering demonstrating the preferred ultrasound plane for measurement of biparietal diameter. Technical parameters: multidetector CT scanner (GE Lightspeed 16, General Electric Healthcare, Chicago Illinois) in helical scan mode, standard reconstruction algorithm, 140kVp, auto mA (300-715), 0.5s rotational speed, pitch 1.75, and 1.25 mm slice thickness [Color figure can be viewed at [wileyonlinelibrary.com](http://wileyonlinelibrary.com)]

*cerebri* centered between the parietal bones (Figure 6; a 3D volume rendering from an archived head CT of a live *Tursiops* demonstrating the preferred ultrasound plane for measurement of biparietal diameter). Calipers were placed at the outer edge of the near-field parietal bone and the inner edge of the far-field parietal bone (Figure 7A).

Fetal thorax diameter at the level of the heart was measured left-to-right in dorsal and transverse planes, and dorsal-to-ventral in a sagittal plane (Figure 7D-F). Fetal position/motion dictated which measurement(s) could be obtained in any given examination.

Aortic diameter, the maximum anechoic distance between aortic walls near the heart (Figure 7B), was obtained in triplicate. Blubber thickness was measured in a sagittal plane at the level of the heart, from the dorsal skin surface to the margin between the hypoechoic blubber and hyperechoic underlying connective tissue (Figure 7C). Maximum orthogonal measurements of the fetal eye spanned the inner margins of the anechoic vitreous body (Figure 8A). Heart rate was assessed in B-mode using triplicate M-mode measurements. Cardiac flicker signified heart movement in an embryo too small to measure rate. Fluid in the forestomach (first gastric chamber in a dolphin) and/or urinary bladder were noted (Figure 8B,D), in addition to peritoneal effusion and any anomalies involving the stomach, kidneys, or liver. Sex was determined if the genitalia could be identified (Figure 8C,D).

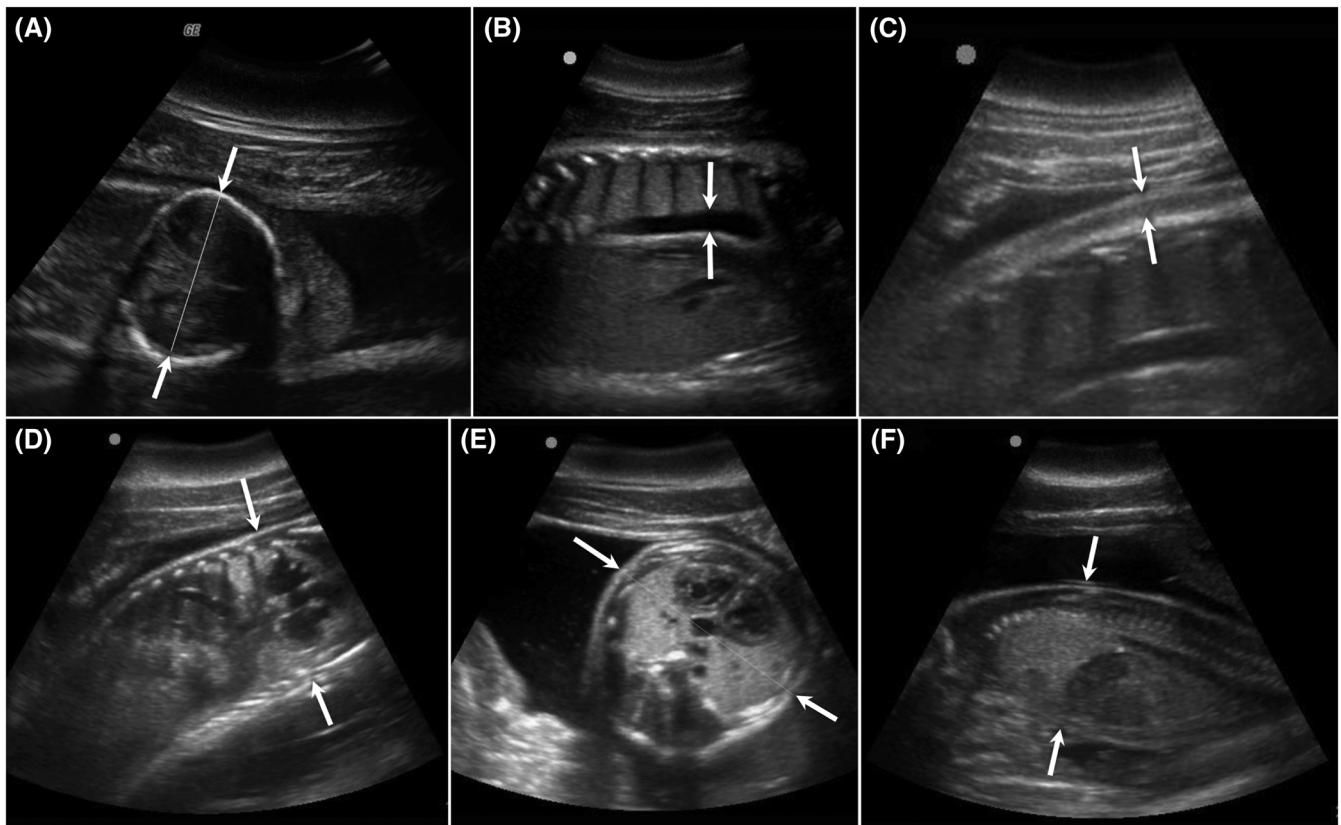


**FIGURE 7** Six fetal parameters that best correlate with gestational age; arrows indicate dimensions of each parameter. A, BPD (dorsal plane), fetal rostrum is to the right. B, Aortic diameter (sagittal), fetal head is to the right and dorsum is in the near field. C, Dorsal blubber thickness (sagittal), fetal head is to the right. D, Thoracic width (dorsal plane), fetus's right is in the near field and head is to the right. E, Thoracic width (transverse), fetal heart is in the right near field. F, Thoracic height (sagittal), fetal head is to the left and dorsum is in the near field (2-5 MHz curvilinear transducer)

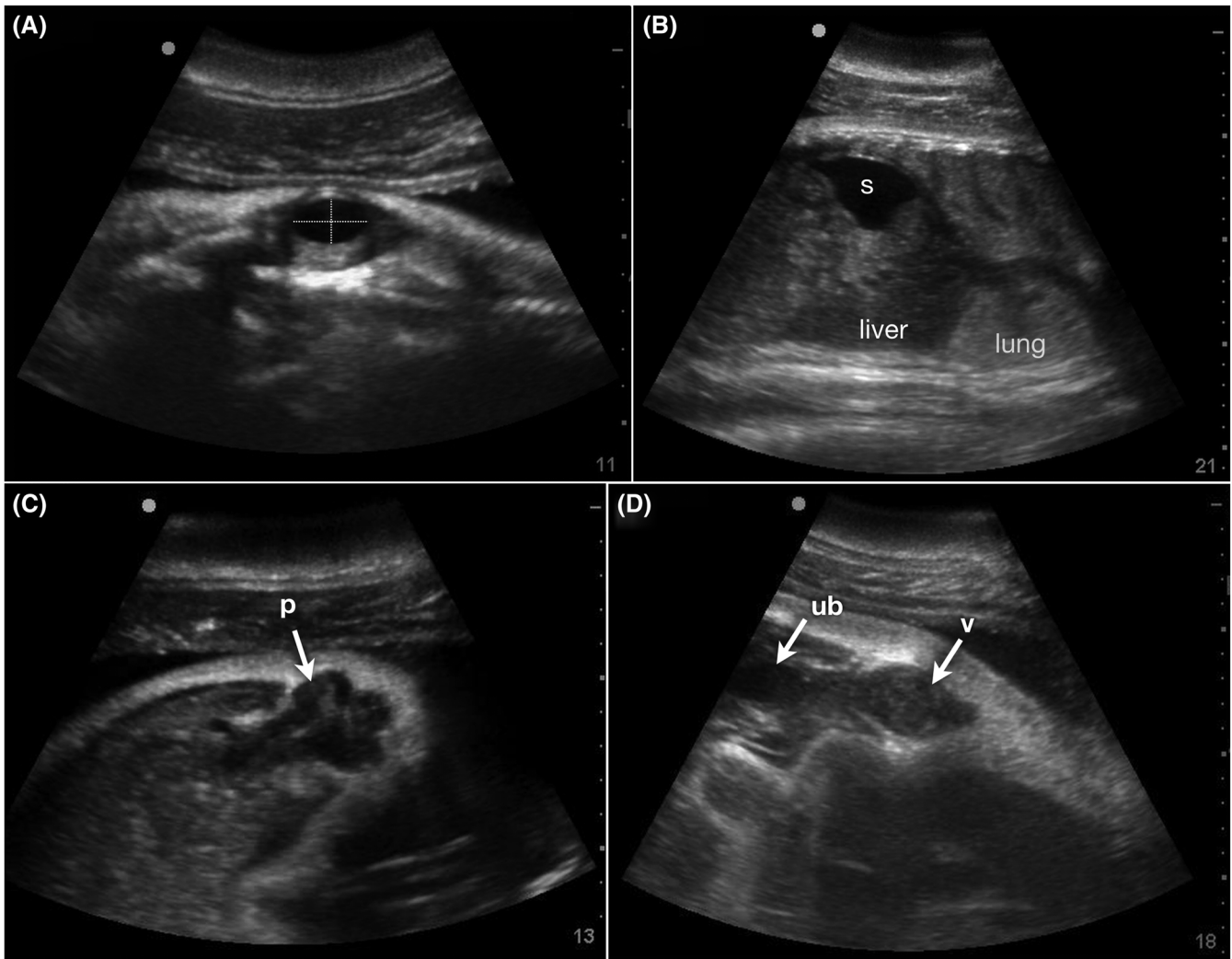


**FIGURE 8** A, Fetal eye (rostrum is to the right). Orthogonal lines indicate dimensions. B, Fetal forestomach(s) containing anechoic fluid. Fetal left is in the near field, head is to the right. C, Male fetal genitalia; sigmoid flexure at base of *Tursiops* penis (p) is evident as a tri-lobed structure; fetal ventrum is in the near field and head is to the right. D, Female fetal genitalia, showing vagina (v) and urinary bladder (ub); fetal left is in the near field and head is to the left (2-5 MHz curvilinear transducer)

Dorsal or sagittal images of lung adjacent to liver were chosen (Figure 9), and organ echogenicity and homogeneity evaluated. One square region of interest was drawn within each organ, generating a mean pixel intensity (MPI) to quantify echogenicity. Regions of interest were of maximum uniform size, chosen at similar depth to minimize the effect of attenuation, and avoided acoustic shadowing (ribs) and areas of enhancement (vessels). The lung/liver MPI ratio was determined. Focal or diffuse lesions and pleural or pericardial effusion were noted. Illustrations of fetomaternal structures in each trimester are shown in Figure 10A-C.

### 2.3 | Statistical analyses

Statistical tests were selected and performed by a veterinarian (A.B.) with graduate-level statistics training (two MS degrees), using statistical analysis freeware (R software 3.3.0. for data analysis, [www.r-project.org](http://www.r-project.org)). Shapiro-Wilk tests for normality and subsequently nonparametric statistical analyses were performed through-

out, including Wilcoxon Signed Rank Test, Mann-Whitney *U* test, and Kruskal-Wallis analysis. A significance of  $P < .05$  was used for all analyses. Simple and quantile regression analysis was performed to assess the relationship of quantitative variables with the stage of gestation. Pearson correlation coefficient evaluated the relationships between fetal measurements and the day of gestation. Assuming a 380-day gestation in *Tursiops*,<sup>15</sup> fetal age was back-calculated from the parturition date, and trimesters divided into three 127-day blocks (first = 0–126 days, second = 127–253 days, and third = 254–380 days).

## 3 | RESULTS

A total of 203 ultrasound examinations were included in the study. Every dam had a single fetus. Up to 70 ultrasonographic parameters were assessed in each scan (see Supporting Information 1 for a sample datasheet).

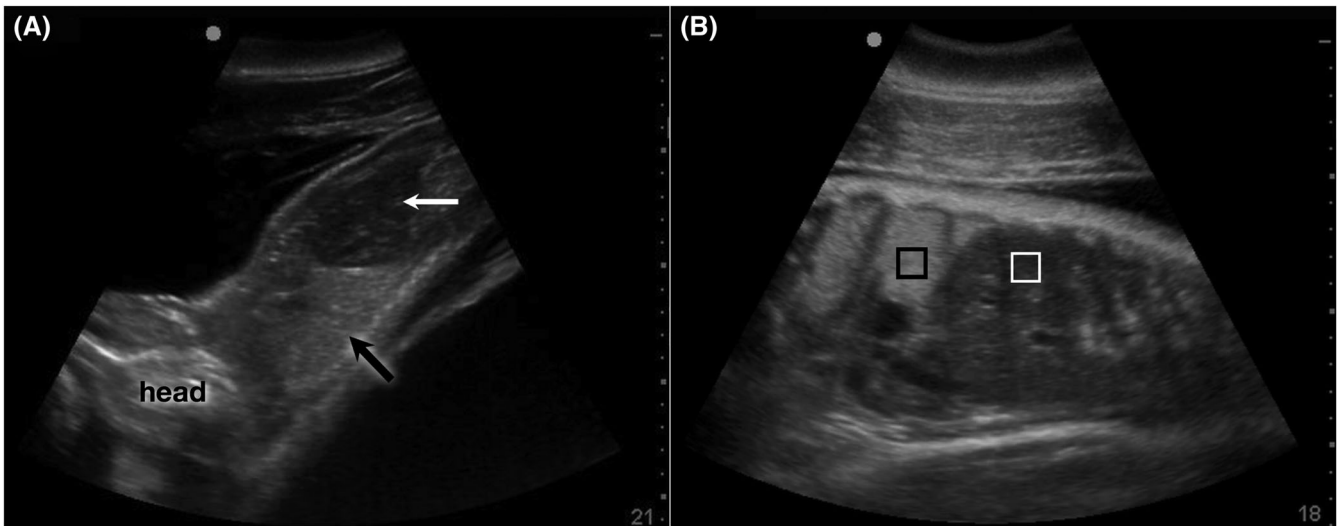


**FIGURE 9** A, Sagittal view of the fetal lung (black arrow) and liver (white arrow). Caudal ventrum of fetus is in the near field. B, Oblique dorsal view; the fetus's dorsum is in the near field. The black square (lung) and white square (liver) denote regions of interest for determination of mean pixel intensity (2-5 MHz curvilinear transducer)

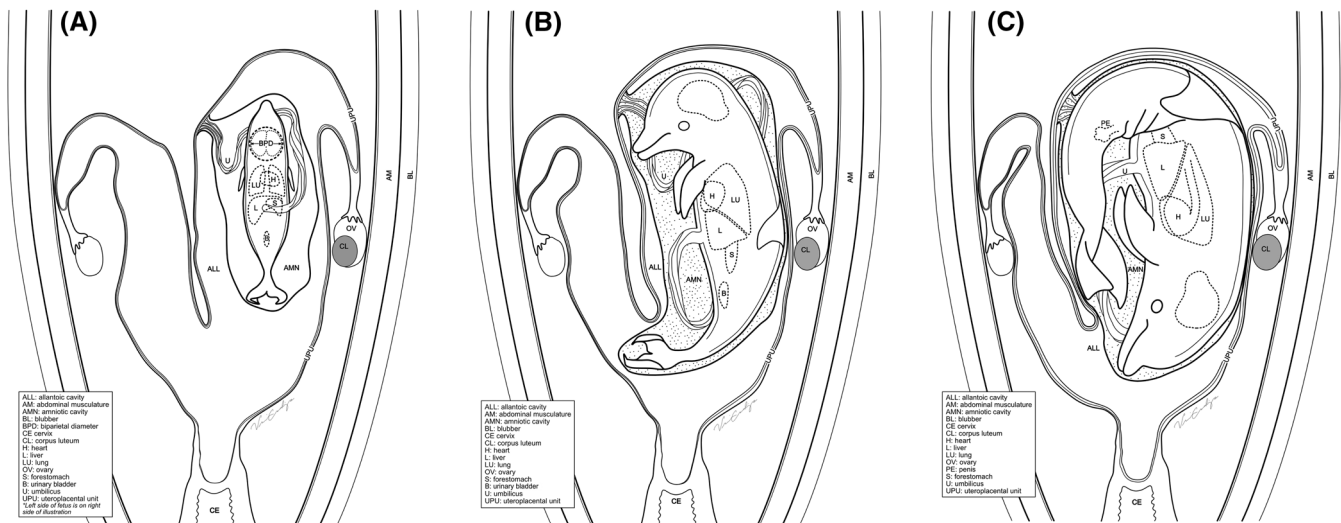


**FIGURE 10** Illustrations of the fetomaternal anatomical structures in the A, first; B, second; and C, third trimester

Nine dams had a left ovarian CL and seven had a right ovarian CL. Maximum CL diameter was 3.7 cm and did not vary based on laterality (right: 2.5-3.7 cm, left: 2.1-3.6 cm). A central anechoic cavity was seen in five of 16 corpora lutea; others were solid. Static cyst-like structures (0.9-3.5 cm diameter) were noted on the gravid-side ovary in four pregnancies of four animals. Cyst laterality was split evenly in these pregnancies. One animal had two cyst-like structures. Other cysts were single. Transient follicles (>3) were detected in the non-CL ovary in three examinations of two dams; both occurred during the first half of gestation.

The uteroplacental unit had a thin layered wall. There was a significant increase in thickness over the course of gestation in all three locations (Table 1). Maximum was 5.6 mm, noted in the caudal region on day 357 of one pregnancy. No abnormalities suggestive of uteroplacental disruption were found. In four dams, echogenic internal roughening

was noted, with/without frond-like projections that extended  $\leq 1$  cm into the lumen (Figure 4B).

Uterine fluid assessment was possible in 148 of 203 examinations. Allantoic and amniotic fluid were distinguishable in 100 of 148 examinations. In all 100, the allantoic fluid was anechoic (Figure 3B). Amniotic fluid was identified in 102 examinations. It was diffusely hyperechoic in 24% (49/102). Echogenic FFPs were only seen in amniotic fluid (25% or 26/102) in the second half of gestation (Figure 4A). Maximum recorded amniotic depth ( $10.4 \pm 2.67$  cm) exceeded allantoic ( $7.8 \pm 2.67$  cm). Fluid depths did not correlate with gestation.

The umbilical cord was examined in 64% ( $n = 130$ ). Four umbilical vessels (two arteries and two veins)<sup>40</sup> were identified in all examinations where the umbilical vasculature was seen in cross section (48%; Figure 5A,B). In this same subset of examinations, the urachus was identified in 46 studies. Cord diameter near the fetal insertion

**TABLE 1** Regional thickness of the uteroplacental unit (UPU) based on trimester

UPU (cm)	First trimester	Second trimester	Third Trimester	P-value
Cranial	0.22–0.31 (8)	0.26–0.29 (37)	0.30–0.32 (50)	<.00011*
Mid	ND	0.29–0.33 (22)	0.33–0.37 (38)	<.00057*
Caudal	0.27–0.31 (7)	0.30–0.33 (33)	0.36–0.40 (45)	<.000011*

Notes. 95% Confidence intervals according to trimester. Sample size (n) differed with location and trimester.

ND, no data.

\*Significantly different by Kruskal-Wallis analysis.

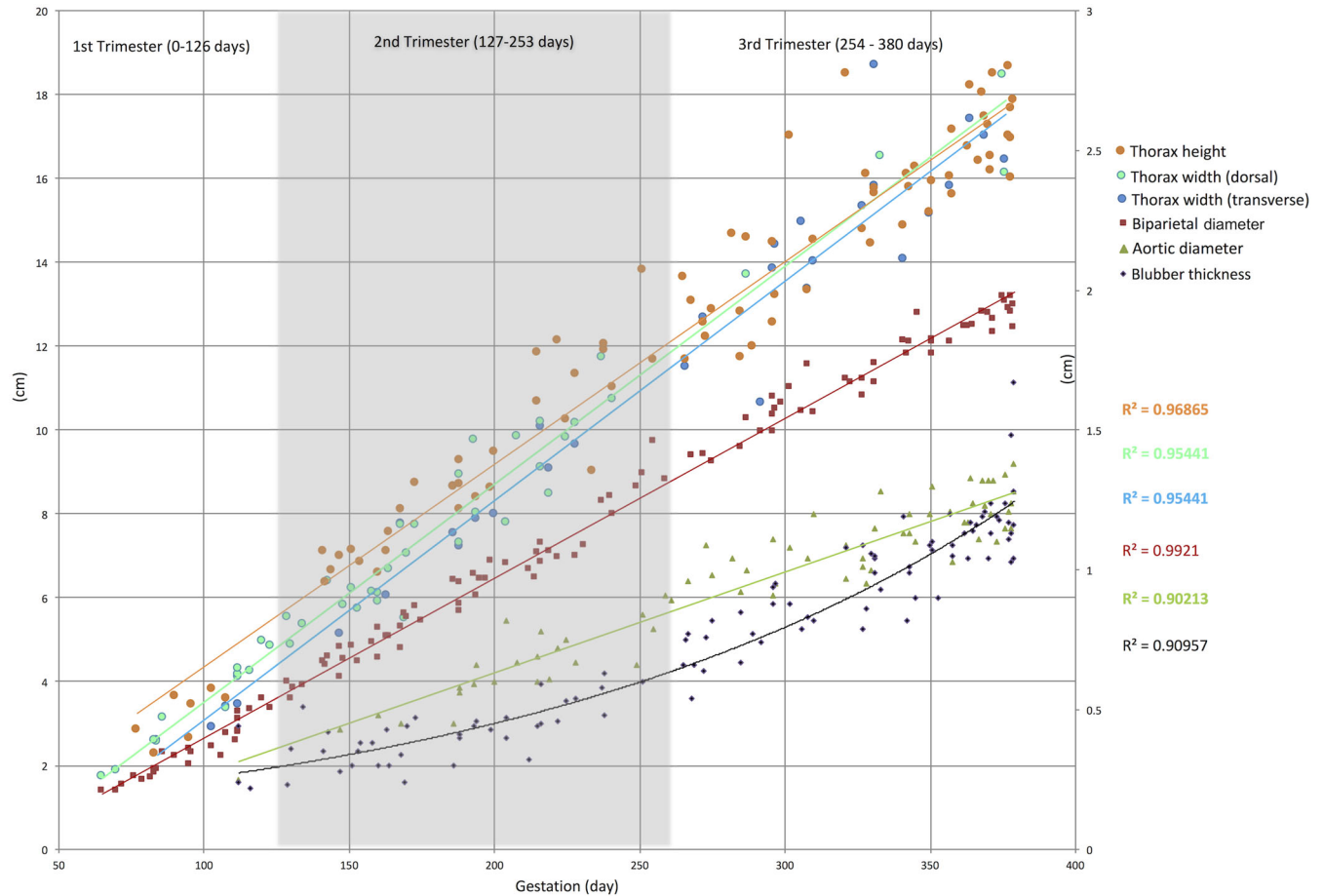


**FIGURE 11** Six ultrasonographic parameters of fetal growth based on day of gestation and trimester [Color figure can be viewed at [wileyonlinelibrary.com](http://wileyonlinelibrary.com)]

was measured in 77 of 130 cord examinations (Figure 5C). Minimum and maximum cord diameter were 1.1 cm (day 95) and 3.9 cm (day 364). Cord diameter was positively correlated with gestational age ( $R^2 = 0.7$ ). In three exams of two animals, a loose, ball-shaped coil was identified in the cord (Figure 5D) that resolved by the following evaluation.

Fetal activity was characterizable in 122 exams. It was frequent in 62%, rare in 32%, and continuous in 6%. One cursory exam performed on gestational day 377 of 380 did not record fetal movement.

Fetal BPD, thoracic width, thoracic height, aortic diameter, and blubber thickness all demonstrated very high correlation with gestational age ( $R^2 > 0.94$ ) (Figure 11). Table 2 serves as a clinical reference for normal growth progression of fetal structures. The strongest linear

correlation ( $P = .00001$ ) with actual fetal age was BPD. Days until parturition =  $348.16 - (26.03 \times \text{BPD})$  is a highly accurate equation of prospective fetal age determination (BPD in cm) ( $R^2 = 0.99$ ). The earliest and latest possible gestational age for six fetal measurements is outlined in Table 3. Fetal eye dimensions were less tightly correlated to gestational age than other parameters ( $R^2 = 0.77, n = 48$ ).

Fetal cardiac motion was recorded in 86% of examinations. Heart rate was normally distributed and had a strong negative correlation with gestation, decreasing during pregnancy. Maximum and minimum rates were 188 bpm (day 120) and 76 bpm (day 379). Rate varied with gestational age as follows: 1st trimester, difficult to assess; 2nd trimester, 118–173 bpm ( $n = 34$ ); 3rd trimester, 76–154 bpm ( $n = 95$ ); last 2 weeks of gestation, 76–125 bpm ( $n = 40$ ). The earliest



cardiac movement was recorded opportunistically on day 70 during a monthly examination. Cardiac flicker was seen in two first-trimester examinations. Correlations were not found between fetal heart rate and activity, nor between activity and gestational age.

Fluid was seen in the fetal forestomach in 42% of exams and the urinary bladder in 41%. The genitalia became conspicuous in 12 of 16 pregnancies; these 12 fetuses were all correctly sexed ultrasonographically (six male, six female).

Fetal lung was discernible from liver as early as day 112, and in all fetuses by the end of the first trimester. Fetal lung was subjectively and objectively hyperechoic to fetal liver (lung MPI =  $87.9 \pm 14.5$  [95% confidence interval 84.7–91.1], liver MPI =  $35.7 \pm 7.1$  [95% confidence interval 34.1–37.2]). Mean pixel intensity did not correlate to gestational age. Lung:liver MPI ratio was  $2.57 \pm 0.46$  (95% confidence interval 2.47–2.67), denoting lung was roughly twice as echogenic as liver. The lung was nearly always homogeneous in echotexture (92%). No anomalies or focal lesions of the fetal calvarium, eyes, blubber, heart, aorta, lungs, pleural space, peritoneum, liver, forestomach, kidneys, urinary bladder, or genitalia were noted.

## 4 | DISCUSSION

This study describes a standardized ultrasound method for obtaining in utero measurements in dolphins. The reference values detailed in these 16 successful pregnancies are reproducible, critical to ultrasonographic assessment of pregnant dolphins, and may facilitate early diagnosis of abnormalities. The highly accurate updated<sup>13</sup> equation presented in this publication for determining gestational age based on biparietal diameter (days to parturition =  $348.16 - (26.03 \times \text{BPD})$ ) aids in timing of clinical decisions as parturition approaches. We also demonstrate that several other fetal measurements (thorax, aorta, blubber) are practical indices to obtain and are highly accurate in predicting gestational age (Figure 11). New equations define the earliest and latest possible day of gestation for each of six fetal measurements (Table 3). In addition, the medical illustrations of dolphin fetomaternal anatomy (Figure 10) presented in this study correlate to ultrasound and further understanding of spatial relationships.

Based on our review of the literature, this study is the first report of the normal ultrasonographic appearance of the *Tursiops* uteroplacental unit. We report normal reference ranges and demonstrate that regional uteroplacental thickness significantly increases with each trimester. Disruption of uteroplacental contact, a sign of placentitis and abnormal separation of the allantochorion from the endometrium,<sup>41</sup> was not seen in any of the successful pregnancies in this study. Significant deviations from the values reported here may aid in diagnosis of placentitis or other placental pathology.

A thorough ultrasonographic evaluation of the reproductive tract should routinely be performed in sexually mature female dolphins. Identification and monitoring of ovarian corpora, developing follicles, and cyst-like lesions establishes baseline "normal" for each animal, detects reproductive cycle changes, and facilitates diagnosis of pregnancy and pathology.

**TABLE 2** Mean fetal ultrasonographic measurements based on month and trimester

Fetal Measurements Month →	n	First trimester (days 0–126)			Second trimester (days 127–253)			Third trimester (days 254–380)			Pre-birth		
		2	3	4	5	6	7	8	9	10		11	12
Aortic diameter (cm)	72	0.02–0.13	0.13–0.23	0.23–0.34	0.34–0.45	0.45–0.56	0.56–0.67	0.67–0.77	0.77–0.88	0.88–0.99	0.99–1.10	1.10–1.21	1.21–1.31
Biparietal diameter (cm)	117	0.01–1.13	1.13–2.27	2.27–3.42	3.42–4.56	4.56–5.70	5.70–6.84	6.84–7.99	7.99–9.13	9.13–10.27	10.27–11.42	11.42–12.56	12.56–13.70
Thorax width dorsal (cm)	45	0.0–1.43	1.43–2.99	2.99–4.55	4.55–6.11	6.11–7.67	7.67–9.23	9.23–10.79	10.79–12.35	12.35–13.91	13.91–15.47	15.47–17.03	17.03–18.59
Thorax height (cm)	84	0.97–2.42	2.42–3.97	3.97–5.32	5.32–6.77	6.77–8.22	8.22–9.67	9.67–11.12	11.12–12.56	12.56–14.01	14.01–15.46	15.46–16.91	16.91–18.36
Blubber thickness (cm)	102	0.17–0.20	0.20–0.24	0.24–0.29	0.29–0.34	0.34–0.40	0.40–0.48	0.48–0.57	0.57–0.67	0.67–0.80	0.80–0.95	0.95–1.13	1.13–1.34

Notes. n, sample size for each measurement.

**TABLE 3** Determination of earliest and latest possible gestational day based on fetal measurements

Fetal Measurement (x)	Earliest Possible Gestational Day (y)	Latest Possible Gestational Day (y)
Aortic Diameter	$y = 278.95x - 24.74$	$y = 281.82x + 63.00$
Biparietal diameter	$y = 23.92x + 31.21$	$y = 26.82x + 41.26$
Thorax width (dorsal)	$y = 16.09x + 35.64$	$y = 19.51x + 61.31$
Thorax width (trans)	$y = 15.35x + 43.93$	$y = 14.53x + 137.08$
Thorax height	$y = 15.82x + 28.38$	$y = 20.95x + 39.07$
Blubber thickness	$y = 211.21x + 26.28$	$y = 236.11x + 140.50$

Notes. Quantile regression threshold equations used to determine 95% confidence intervals.

x, fetal measurement; y, day in gestation.

Echogenic particles in amniotic fluid of human fetuses can indicate the presence of vernix (shedding of fetal skin), and are also seen in the allantoic fluid of healthy pregnant mares within 10 days of foaling.<sup>29</sup> Echogenic particles or FFPs may indicate pathology and fetal stress when associated with infective debris, blood, or meconium;<sup>42</sup> however, increased fluid echogenicity is not always predictive of pathology.<sup>43</sup> No allantoic FFPs were seen in our study, but they were noted in amniotic fluid. In light of the successful pregnancy outcomes for these animals and lack of findings indicative of fetal stress, we suspect the presence of amniotic echogenic particles may be normal in *Tursiops*.

The finding of a ball-shaped umbilical coil in three of 203 exams in our study was surprising, given the focally convoluted appearance of the cord and the clinical concern warranted for antenatal diagnosis of true umbilical knots in humans<sup>39</sup> and neonatal dolphins.<sup>44</sup> A convoluted or tangled cord, sometimes found in monoamniotic twin pregnancies in women, was not anticipated in this species (twins are exceedingly rare in dolphins). Given that both coils resolved and no clinical sequela resulted, we suggest this may be transiently seen in a normal pregnancy.

Some limitations in our study are worth noting. The sample size (16 pregnancies) is relatively low, but this should be weighed against the complexity involved in gaining longitudinal access to long-lived, legislatively protected animals such as dolphins and the value of acquiring such data.<sup>45</sup> Behavioral cooperation of the dam and position of the fetus during any given exam dictated the quality/quantity of data acquired. In addition, the retrospective nature of image analysis despite prospective image acquisition necessarily resulted in dataset truncation. Not all measurements could be derived from each set of captured cine and still images. With regards to fetal fluid depths, for example, measurements obtained may not have represented the deepest fluid pocket present but rather the greatest depth captured in the exam. The lack of correlation between fetal fluid depth and gestational age in dolphins has also been found in horses.<sup>31</sup> Clinically, it may be of most value to note the fluid characteristics reported and maximum fluid depths seen in these successful pregnancies. Retrospective assessment of fetal movement was also limiting. The inability to evaluate activity in 40% of exams was likely due to inadequate recording of fetal motion during abbreviated scans. Further, the compression of the

fetus by the fusiform, hydrodynamic abdomen of a cetacean, also limits its movement near term. Anecdotally, fetal movement was always seen in first or second trimester evaluations. In general, a multifactorial approach is essential to pregnancy evaluation, as a single abnormal parameter may not be representative of the overall clinical state. Lack of fetal movement during a given exam may not indicate lack of fetal viability, however if coupled with undetectable cardiac motion, abnormalities in organ conspicuity or echogenicity, or abnormal fetometrics, this likely represent fetal loss.<sup>46</sup>

The simplified use of MPI as a proxy for echogenicity<sup>47</sup> rather than gray level histogram width assessment<sup>48</sup> or gray-scale histogram<sup>49</sup> is also a limitation. However, the importance of establishing the normal ultrasonographic appearance of fetal dolphin lung and its relationship to liver in light of recent reports of fetal pneumonia and perinatal mortality in wild dolphins necessitated straightforward, reproducible methodology. Dolphin fetal lung in our study, as expected, was largely homogeneous and hyperechoic to liver due to a high density of fluid-tissue interfaces.<sup>2</sup> Lung lesions in human fetuses are generally echogenic.<sup>50,51</sup> None were seen in this study. Normal fetal lung and lung/liver echogenicity relationships facilitate early diagnosis of congenital bronchopulmonary abnormalities in human fetuses, and a decrease in the fetal lung:liver echogenicity has been shown to predict respiratory distress in newborns.<sup>49</sup> As such, comparison of fetal dolphin lung:liver MPI to values published here could enable future identification of respiratory pathology in perinatal dolphins.

In conclusion, this study provides reference information on the qualitative and quantitative fetomaternal ultrasonographic findings associated with successful pregnancy in bottlenose dolphins. This information may be used as the basis for identifying gestational abnormalities in managed populations and their wild counterparts. Lesions affecting morbidity or mortality of the fetus or dam detected early could result in timely therapeutic intervention for animals in human care, and findings indicating reproductive failure in the wild may be elucidated. Additional studies are needed to corroborate our findings, expand the dataset, and apply these diagnostic imaging methods to other cetacean species of interest.

## LIST OF AUTHOR CONTRIBUTIONS

### Category 1

- Conception and Design: Ivančić, Smith, Gomez, Meegan
- Acquisition of Data: Ivančić, Smith, Gomez, Meegan, Musser, Cárdenas Llerenas, Waitt
- Analysis and Interpretation of Data: Ivančić, Smith, Gomez, Meegan, Musser, Barratclough, Jensen

### Category 2

- Drafting the Article: Ivančić, Musser, Barratclough
- Revising Article for Intellectual Content: Ivančić, Smith, Gomez, Meegan, Musser, Barratclough, Jensen, Cárdenas Llerenas, Waitt

### Category 3

- (a) Final Approval of the Completed Article: Ivančić, Smith, Gomez, Meegan, Musser, Barratclough, Jensen, Cárdenas Llerenas, Waitt

### ACKNOWLEDGMENTS

The authors thank Veronica Cendejas for her technical expertise and dedication in creating the anatomical drawings in this text. This research was made possible by a grant from The Gulf of Mexico Research Initiative (GoMRI), Award SA 16–17. Data are publicly available through the Gulf of Mexico Research Initiative Information & Data Cooperative (GRIIDC) at <https://data.gulfresearchinitiative.org> (<https://doi.org/10.7266/n7-eydg-cy02>).

### CONFLICT OF INTEREST

The authors declare no potential conflicts of interest with respect to the research, authorship, and/or publication of this article.

### ORCID

Marina Ivančić  <https://orcid.org/0000-0003-2289-8926>

### REFERENCES

- Luck CA. Value of routine ultrasound scanning at 19 weeks: A four year study of 8849 deliveries. *Br Med J*. 1992;304(6840):1474-1478.
- Achiron R, Strauss S, Seidman DS, Lipitz S, Mashiach S, Goldman B. Fetal lung hyperechogenicity: Prenatal ultrasonographic diagnosis, natural history and neonatal outcome. *Ultrasound Obstet Gynecol*. 1995;6(1):40-42.
- Smith CR, Solano M, Lutmerding BA, et al. Pulmonary ultrasound findings in a bottlenose dolphin *Tursiops truncatus* population. *Dis Aquat Organ*. 2012;101(3):243-255.
- Sklansky M, Levine G, Havlis D, et al. Echocardiographic evaluation of the bottlenose dolphin (*Tursiops truncatus*). *J Zoo Wildl Med*. 2006;37(4):454-463.
- Brook FM. Ultrasonographic imaging of the reproductive organs of the female bottlenose dolphin. *Tursiops truncatus aduncus* *Reproduction*. 2001;121(3):419-428.
- Seitz KE, Smith CR, Marks SL, Venn-Watson SK, Ivančić M. Liver ultrasonography in dolphins: Use of ultrasonography to establish a technique for hepatobiliary imaging and to evaluate metabolic disease-associated liver changes in bottlenose dolphins (*Tursiops truncatus*). *J Zoo Wildl Med*. 2016;47(4):1034-1043.
- Smith CR, Venn-Watson S, Wells RS, et al. Comparison of nephrolithiasis prevalence in two bottlenose dolphin (*Tursiops truncatus*) populations. *Front Endocrinol*. 2013;4:145.
- Fiorucci L, García-Párraga Macrelli R, Grande F, et al. Determination of the main reference values in ultrasound examination of the gastrointestinal tract in clinically healthy bottlenose dolphins (*Tursiops truncatus*). *Aquat Mamm*. 2015;41(3):284-294.
- Martony ME, Ivančić M, Gomez FM, et al. Establishing marginal lymph node ultrasonographic characteristics in healthy bottlenose dolphins (*Tursiops truncatus*). *J Zoo Wildl Med*. 2017;48(4):961-971.
- Jensen ED. Embryonic/early fetal loss in the Atlantic bottlenose dolphin. Paper presented at: Bottlenose Dolphin Reproduction Workshop 1999; June 3–6, 1999; San Diego, CA, USA.
- Lacave G, Eggermont M, Verslycke T, et al. Prediction from ultrasonographic measurements of the expected delivery date in two species of bottlenose dolphin (*Tursiops truncatus* and *Tursiops aduncus*). *Vet Rec*. 2004;154(8):228-233.
- Robeck TR, Gili C, Doescher BM, et al. Altrenogest and progesterone therapy during pregnancy in bottlenose dolphins (*Tursiops truncatus*) with progesterone insufficiency. *J Zoo Wildl Med*. 2012;43(2):296-308.
- Neuenhoff RD, Cowan DF, Whitehead H, Marshall CD. Prenatal data impacts common bottlenose dolphin (*Tursiops truncatus*) growth parameters estimated by length-at-age curves. *Mar Mam Sci*. 2011;27(1):195-216.
- Wells RS, Smith CR, Sweeney JC, et al. Fetal survival of common bottlenose dolphins (*Tursiops truncatus*) in Sarasota Bay, Florida. *Aquat Mamm*. 2014;40(3):252.
- Smith CR, Jensen ED, Blankenship BA, et al. Fetal omphalocele in a common bottlenose dolphin (*Tursiops truncatus*). *J Zoo Wildl Med*. 2013;44(1):87-92.
- García-Párraga D, Brook F, Crespo-Picazo JL, et al. Recurrent umbilical cord accidents in a bottlenose dolphin *Tursiops truncatus*. *Dis Aquat Organ*. 2014;108(2):177-180.
- Gray KN, Conklin RH. Multiple births and cardiac anomalies in the bottle-nosed dolphin. *J Wildl Dis*. 1974;10(2):155-157.
- Brook FM. Ultrasound diagnosis of anencephaly in the fetus of a bottlenose dolphin (*Tursiops aduncus*). *J Zoo Wildl Med*. 1994;25(4):569-574.
- Colegrove KM, Venn-Watson S, Litz J, et al. Fetal distress and in utero pneumonia in perinatal dolphins during the Northern Gulf of Mexico unusual mortality event. *Dis Aquat Organ*. 2016;119(1):1-6.
- Schwacke LH, Smith CR, Townsend FI, et al. Health of common bottlenose dolphins (*Tursiops truncatus*) in Barataria Bay, Louisiana, following the Deepwater Horizon oil spill. *Environ Sci Technol*. 2014;48(1):93-103.
- Kellar NM, Speakman TR, Smith CR, et al. Low reproductive success rates of common bottlenose dolphins *Tursiops truncatus* in the northern Gulf of Mexico following the Deepwater Horizon disaster (2010-2015). *Endang Species Res*. 2017;33:143-158.
- Lane SM, Smith CR, Mitchell J, et al. Reproductive outcome and survival of common bottlenose dolphins sampled in Barataria Bay, Louisiana, USA, following the Deepwater Horizon oil spill. *Proc R Soc B*. 2015;282(1818):20151944.
- Smith CR, Rowles TK, Hart LB, et al. Slow recovery of Barataria Bay dolphin health following the Deepwater Horizon oil spill (2013-2014), with evidence of persistent lung disease and impaired stress response. *Endanger Species Res*. 2017;33:127-142.
- Venn-Watson S, Colegrove KM, Litz J, et al. Adrenal gland and lung lesions in Gulf of Mexico common bottlenose dolphins (*Tursiops truncatus*) found dead following the Deepwater Horizon oil spill. *PLoS One*. 2015;10(5):e0126538.
- American Institute of Ultrasound in Medicine. AIUM practice guideline for the performance of obstetric ultrasound examinations. *J Ultrasound Med*. 2013;32(6):1083.
- Manning FA, Platt LD, Sapos L. Antepartum fetal evaluation: Development of a fetal biophysical profile. *Am J Obstet Gynecol*. 1980;136(6):787-795.
- Reef VB, Vaala WE, Worth LT, Spencer PA, Hammett B. Ultrasonographic evaluation of the fetus and intrauterine environment in healthy mares during late gestation. *Vet Radiol Ultrasound*. 1995;36(6):533-541.
- Reef VB, Vaala WE, Worth LT, Sertich PL, Spencer PA. Ultrasonographic assessment of fetal well-being during late gestation: Development of an equine biophysical profile. *Equine Vet J*. 1996;28(3):200-208.
- Adams-Brendemuehl C, Pipers FS. Antepartum evaluations of the equine fetus. *J Reprod Fertil*. 1987;35:565-573.

30. Murase H, Endo Y, Tsuchiya T, et al. Ultrasonographic evaluation of equine fetal growth throughout gestation in normal mares using a convex transducer. *J Vet Med Sci.* 2014;76(7):947-953.
31. Bucca S, Fogarty U, Collins A, Small V. Assessment of feto-placental well-being in the mare from mid-gestation to term: Transrectal and transabdominal ultrasonographic features. *Theriogenology.* 2005;64(3):542-557.
32. Wislocki GB, Enders RK. The placentation of the bottle-nosed porpoise (*Tursiops truncatus*). *Am J Anat.* 1941;68(1):97-125.
33. Samuel CA, Allen WR, Steven DH. Studies on the equine placenta II. Ultrastructure of the placental barrier. *J Reprod Infertil.* 1976;48(2):257-264.
34. Stone LR, Sweeney JC. Ultrasonography of bottlenose dolphins in pregnancy. Paper presented at: IAAAM Conference 1995; May 6–10 1995; Mystic, CT, USA.
35. Stone LR. Fetal ultrasonography with emphasis on fetal development, gestational aging, and physiological assessment. Paper presented at: Bottlenose Dolphin Reproduction Workshop 1999; June 3–6, 1999; San Diego, CA, USA.
36. Williamson P, Gales NJ, Lister S. Use of real-time B-mode ultrasound for pregnancy diagnosis and measurement of fetal growth rate in captive bottlenose dolphins (*Tursiops truncatus*). *J Reprod Fertil.* 1990;88(2):543-548.
37. Raio L, Ghezzi F, Di Naro E, et al. Prenatal diagnosis of a lean umbilical cord: a simple marker for the fetus at risk of being small for gestational age at birth. *Ultrasound Obstet Gynecol.* 1999;13(3):176-180.
38. Weissman A, Jakobi P, Bronshtein M, Goldstein I. Sonographic measurements of the umbilical cord and vessels during normal pregnancies. *J Ultrasound Med.* 1994;13(1):11-14.
39. Bosselmann S, Mielke G. Sonographic assessment of the umbilical cord. *Geburtshilfe Frauenheilkd.* 2015;75(8):808.
40. Benirschke K. Comparative Placentation. <http://placentation.ucsd.edu/dolph.html>. Accessed September 01, 2018.
41. Bailey CS, Heitzman JM, Buchanan CN, et al. B-mode and Doppler ultrasonography in pony mares with experimentally induced ascending placentitis. *Equine Vet J.* 2012;44:88-94.
42. Devore GR, Platt LD. Ultrasound appearance of particulate matter in amniotic cavity: Vernix or meconium. *J Clin Ultra.* 1986;14(3):229-230.
43. Tam G, Al-Dughhaishi T. Case report and literature review of very echogenic amniotic fluid at term and its clinical significance. *Oman Med J.* 2013;28(6).
44. Tanaka M, Izawa T, Kuwamura M, et al. A case of meconium aspiration syndrome in a bottlenose dolphin (*Tursiops truncatus*) calf. *J Vet Med Sci.* 2014;76(1):81-84.
45. Olea-Popelka F, Rosen LE. A practical guide for statistics in wildlife studies. In: Miller ER, Lamberski N, Calle P, eds. *Fowler's Zoo and Wild Animal Medicine: Current Therapy.* St. Louis, MO: Elsevier Health Sciences; 2018:21-27.
46. Davidson AP, Nyland TG, Tsutsui T. Pregnancy diagnosis with ultrasound in the domestic cat. *Vet Radiol.* 1986;27(4):109-114.
47. Ivančić M, Mai W. Qualitative and quantitative comparison of renal vs. hepatic ultrasonographic intensity in healthy dogs. *Vet Radiol Ultrasound.* 2008;49(4):368-373.
48. Maeda K, Utsu M, Yamamoto N, Serizawa M. Echogenicity of fetal lung and liver quantified by the grey-level histogram width. *Ultrasound Med Biol.* 1999;25(2):201-208.
49. Beck AP, Araujo Junior E, Leslie AT, Camano L, Moron AF. Assessment of fetal lung maturity by ultrasound: Objective study using gray-scale histogram. *J Matern-Fetal Neo M.* 2015;28(6):617-622.
50. Achiron R, Hegesh J, Yagel S. Fetal lung lesions: A spectrum of disease. New classification based on pathogenesis, two-dimensional and color Doppler ultrasound. *Ultrasound Obstet Gynecol.* 2004;24(2):107-114.
51. Quinton AE, Smoleniec JS. Congenital lobar emphysema—the disappearing chest mass: Antenatal ultrasound appearance. *Ultrasound Obstet Gynecol.* 2001;17(2):169-171.

## SUPPORTING INFORMATION

Additional supporting information may be found online in the Supporting Information section at the end of the article.

**How to cite this article:** Ivančić M, Gomez FM, Musser WB, et al. Ultrasonographic findings associated with normal pregnancy and fetal well-being in the bottlenose dolphin (*Tursiops truncatus*). *Vet Radiol Ultrasound.* 2020;61:215–226. <https://doi.org/10.1111/vru.12835>